

Effects of vanadium and manganese concentrations on the composition, structure and electrical properties of ZnO-rich MnO_2 – V_2O_5 –ZnO varistors

Heriberto Pfeiffer, Kevin M. Knowles*

Department of Materials Science and Metallurgy, University of Cambridge, Pembroke Street, Cambridge CB2 3QZ, UK

Abstract

The composition, structure and electrical properties of ZnO-rich MnO_2 – V_2O_5 –ZnO varistors have been analysed. Samples were prepared by a conventional powder route with 0.25–0.75 V_2O_5 mol% and 0.1–1.5 MnO_2 mol% concentrations. All the microstructures consisted of ZnO grains with zinc vanadates as minority secondary phases. The quantity and type of zinc vanadates found depended on the cooling rate. α - $\text{Zn}_3(\text{VO}_4)_2$ and $\text{Zn}_4\text{V}_2\text{O}_9$ were found in air-cooled samples, whereas γ - $\text{Zn}_3(\text{VO}_4)_2$ and $\text{Zn}_4\text{V}_2\text{O}_9$ were found in samples cooled relatively slowly at 5°C min^{-1} . All samples exhibited non-linear current-voltage varistor behavior, with non-linear coefficients, α , ranging from 9.7 to 27.3. The electrical behaviour was relatively insensitive to the different rates of cooling. The highest values of α were obtained in slowly cooled samples when the MnO_2 concentration was 0.25 mol% and when the V_2O_5 concentration was 0.5 mol%.

© 2003 Elsevier Ltd. All rights reserved.

Keywords: Electrical properties; Electron microscopy; Powders-solid state reaction; Varistors; ZnO

1. Introduction

Zinc oxide varistor ceramics are technologically important because of their non-linear current-voltage behaviour.¹ In such materials small amounts of oxides other than zinc oxide are added to control the electrical characteristics of the zinc oxide grain boundaries, and thus to optimize the varistor behaviour. While most commercial zinc oxide varistor compositions are based on multi-oxide formulations containing either bismuth oxide or praseodymium oxide in the starting ingredients,¹ it has also been found that simple three oxide formulations based on the addition of small amounts of vanadium and manganese oxides together to zinc oxide can produce good varistor behaviour with non-linear coefficients, α , in excess of 20.^{2–4} Such a relatively simple ternary system is useful both for the study of the

basic science of varistor behaviour and for the systematic study of the effect of process parameters on varistor behaviour. It is also an attractive system to investigate because these varistors can be sintered successfully at relatively low temperatures around 900°C .

In this work, we have extended our previous work in this area³ to examine in more detail the composition, structural characteristics and electrical properties of ZnO-rich V_2O_5 – MnO_2 –ZnO ceramics sintered at 900°C as a function of the V_2O_5 and MnO_2 contents and the rate of cooling to room temperature from 900°C .

2. Experimental procedure

ZnO varistors were synthesised using high purity powders of ZnO (Aldrich), V_2O_5 (Aldrich) and MnO_2 (Aldrich). All the powders were mixed in a ball-milled reactor for 20 h in deionised water using zirconia beads as the dispersion agent. After this the samples were dried, pressed into 10 mm diameter pellets and sintered for 4 h at 900°C . One set of samples was air-cooled to room temperature. A second set of samples was furnace

* Corresponding author. Tel.: +44-1223-334312; fax: +44-1223-334567.

E-mail address: kmk10@cam.ac.uk (K.M. Knowles).

cooled at $5\text{ }^{\circ}\text{C min}^{-1}$ to room temperature. The samples were prepared using different V_2O_5 and MnO_2 molar percentages. V_2O_5 was added at levels of 0.25, 0.5 and 0.75 mol%, while the amounts of MnO_2 used ranged between 0.1 and 1.5 mol%.

The samples were characterised by X-ray diffraction (XRD), scanning electron microscopy (SEM) and transmission electron microscopy (TEM). For XRD a Philips PW-1710 diffractometer coupled to a copper anode X-ray tube was used. The relative percentages of the compounds were estimated from the areas under the diffraction peaks. Sample microstructures were exam-

ined by SEM (JSM-5800LV). TEM samples were also prepared using standard ion beam thinning methods and examined with a JEOL 200CX transmission electron microscope.

3. Results and discussion

A typical XRD pattern from the ZnO-rich V_2O_5 – MnO_2 –ZnO ceramics is shown in Fig. 1(a). A slower, detailed, scan was necessary to enable the various secondary phases to be identified. In all the ceramics examined, ZnO was the main phase and only very small quantities of secondary phases were detected, making an unambiguous identification of the relative proportions of the secondary phases difficult. Nevertheless, in agreement with our previous work,^{3,5} these secondary phases were found to be zinc vanadates. Brown and Hummel⁶ identified three zinc orthovanadates, $\text{Zn}_3(\text{VO}_4)_2$, which they designated as α , β and γ . The α phase (JCPDS file card numbers 29-1396 and 34-0378) is known to be orthorhombic.⁷ Our recent work has shown that the β polymorph is actually the monoclinic phase $\text{Zn}_4\text{V}_2\text{O}_9$ (JCPDS file card number 77-1757), and that the monoclinic γ polymorph (JCPDS file card number 19-1470) is able to incorporate significant amounts of manganese.⁵ These phases were all identified in our samples using the JCPDS file card data, although it should be noted that the identification of the monoclinic γ polymorph on this basis is not definitive (see the discussion in the paper by Hng et al.).⁵ In contrast to the identification of vanadates in these samples, manganese-rich phases were not detected.

The particular vanadium-containing phases present changed as a function of the cooling rate. When the samples were air cooled, α - $\text{Zn}_3(\text{VO}_4)_2$, the polymorph identified by Brown and Hummel as being the low temperature zinc orthovanadate polymorph, was always found. In addition, $\text{Zn}_4\text{V}_2\text{O}_9$ was detected in samples containing MnO_2 concentrations at and above 0.5 mol%. In contrast to this, pellets cooled down relatively slowly at $5\text{ }^{\circ}\text{C min}^{-1}$ always contained γ - $\text{Zn}_3(\text{VO}_4)_2$ instead of α - $\text{Zn}_3(\text{VO}_4)_2$. $\text{Zn}_4\text{V}_2\text{O}_9$ appeared in these samples if the MnO_2 concentration was at or above 0.25 mol%. The possibility therefore arises from these results that both the phases designated here as α - $\text{Zn}_3(\text{VO}_4)_2$ and $\text{Zn}_4\text{V}_2\text{O}_9$ through the JCPDS file cards are also able to incorporate manganese ions into their crystal structures. The trends seen in samples containing 0.25 mol% V_2O_5 are shown in Fig. 1(b) and (c).

SEM and X-ray mapping of the samples confirmed that the varistor samples had a morphology in which vanadium was found at triple junctions and grain boundaries, whereas the manganese was distributed uniformly throughout the samples, such as in the example shown in Fig. 2. These results are consistent

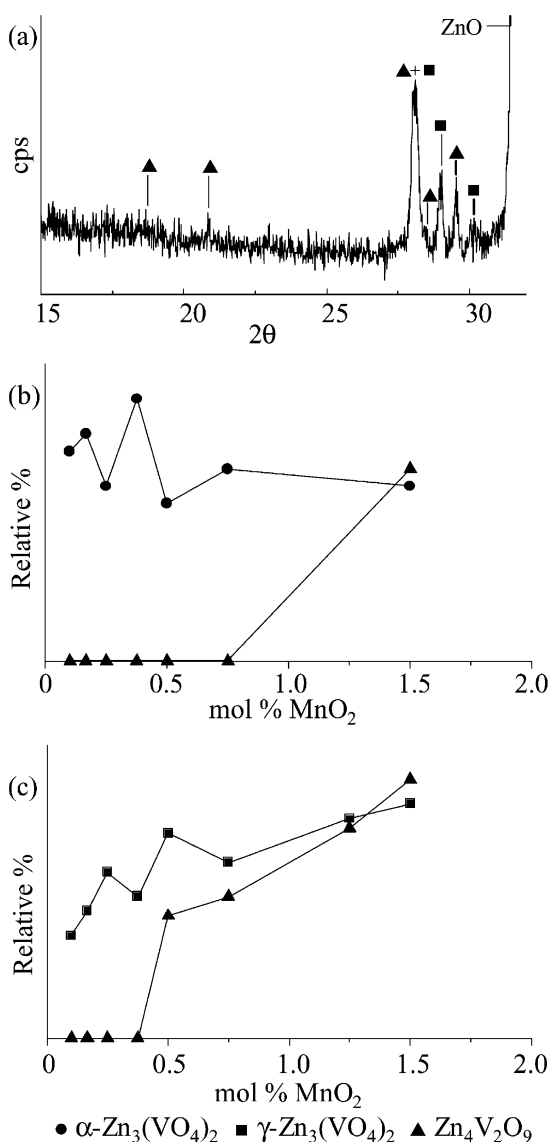


Fig. 1. (a) X-ray diffraction pattern using a step size of $\Delta(2\theta)=0.015^{\circ}$, with a step time of 4 s of the sample containing 0.25 mol% V_2O_5 and 1.25 mol% MnO_2 cooled down at $5\text{ }^{\circ}\text{C min}^{-1}$; (b) plot of the relative proportions of the secondary phases as a function of mol% MnO_2 in the air-cooled 0.25 mol% V_2O_5 samples; (c) plot of the relative proportions of the secondary phases as a function of mol% MnO_2 in the 0.25 mol% V_2O_5 samples cooled down at $5\text{ }^{\circ}\text{C min}^{-1}$.

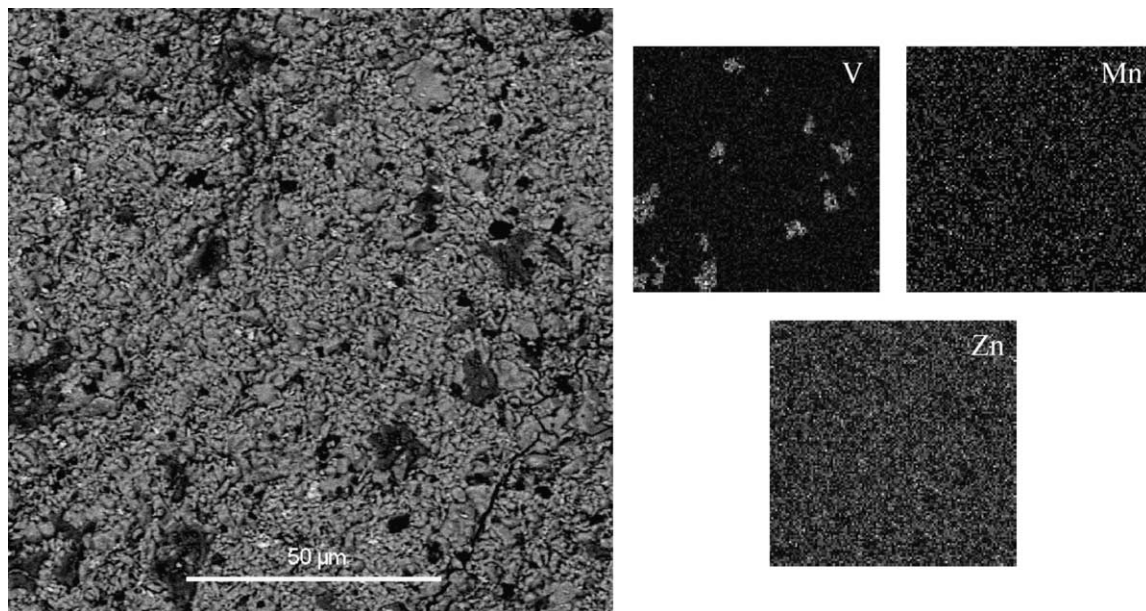


Fig. 2. SEM back-scattered micrograph of the sample containing 0.5 mol% V_2O_5 and 0.1 mol% MnO_2 cooled down at $5^\circ C\ min^{-1}$ together with X-ray maps from vanadium, manganese and zinc. The dark regions have a lower mean atomic number than the average and are vanadium-rich phases. Note that the manganese appears to be distributed uniformly across the sample, implying that it is also incorporated into the vanadium-rich phases.

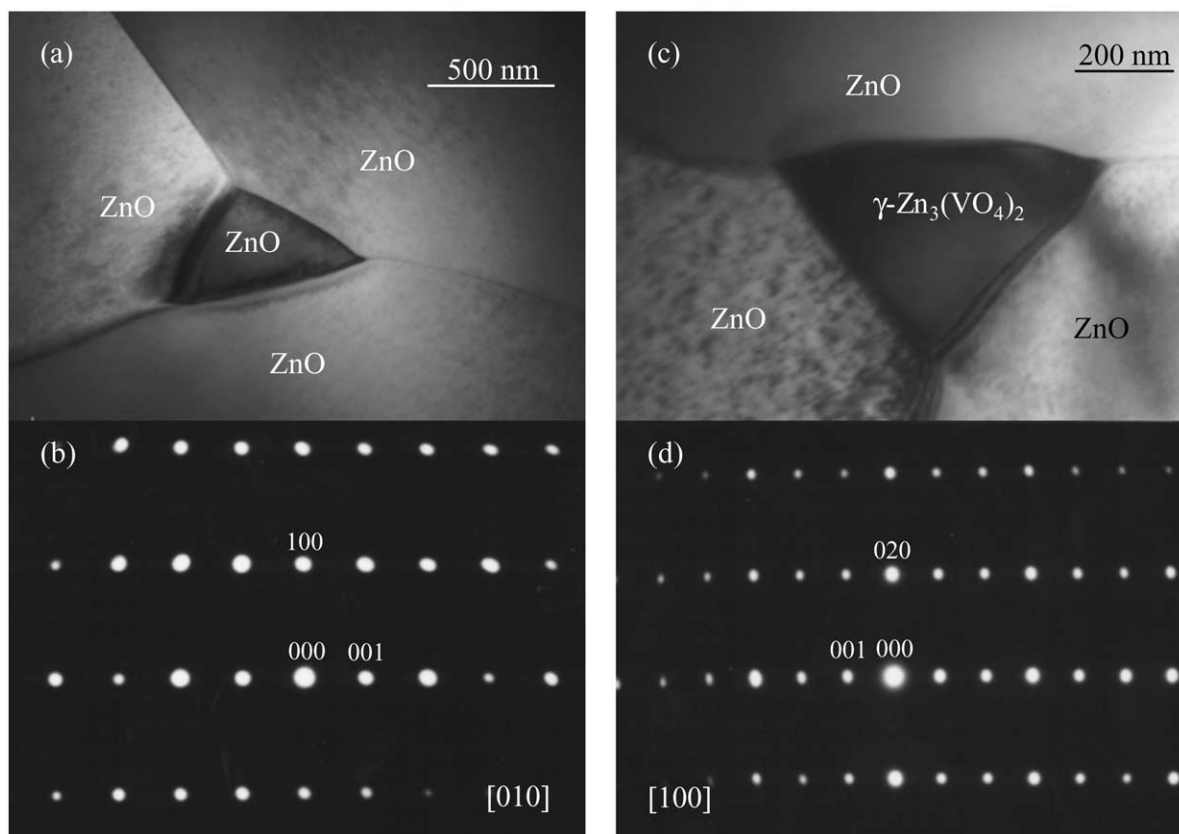


Fig. 3. TEM micrographs and electron diffraction patterns from grains at zinc oxide triple junctions: (a) bright field image of a small ZnO grain from a sample containing 0.5 mol% V_2O_5 and 0.166 mol% MnO_2 cooled down at $5^\circ C\ min^{-1}$, (b) electron diffraction pattern from the [010] zone of the small ZnO grain in (a), (c) bright field image of $\gamma\text{-Zn}_3(\text{VO}_4)_2$ from an air-cooled sample containing 0.5 mol% V_2O_5 and 0.25 mol% MnO_2 and (d) electron diffraction pattern from the [100] zone of $\gamma\text{-Zn}_3(\text{VO}_4)_2$ grain in (c).

with previous work. Grain sizes estimated using standard procedures⁸ were typically in the range 14 ± 3 μm . TEM readily confirmed the existence of vanadates at triple junctions, but also the presence of small ZnO grains. Two examples of phases found at triple junctions are shown in Fig. 3.

The electrical properties of the ZnO-rich V_2O_5 – MnO_2 –ZnO pellets were characterised by their electrical field-current density (E – J) properties. For the 21 samples cooled at 5°C min^{-1} taken as a group, the average breakdown field, E_{break} , measured at 1 mA cm^{-2} current density was 955 V cm^{-1} , with a standard deviation of 190 V cm^{-1} . No systematic trends in the breakdown field and leakage current density, J_{leak} , could be extracted when these two quantities were plotted as a function of vanadium and manganese contents. The average J_{leak} measured at $0.8 E_{\text{break}}$ was $280 \mu\text{A cm}^{-2}$ with a standard deviation of $120 \mu\text{A cm}^{-2}$ and the average non-linear coefficient, α , was 15.3 with a standard deviation of 3.8.

The corresponding values for the 21 air-cooled samples were $1020 \pm 185 \text{ V cm}^{-1}$, $250 \pm 100 \mu\text{A cm}^{-2}$ and 16.2 ± 2.7 . Graphs of the non-linear coefficient, α , as a function of composition and cooling rate are shown in Fig. 4. Encouragingly, α values in excess of twenty are readily obtainable for both air cooling and cooling at 5°C min^{-1} , with the highest value of α found in the samples containing 0.25 mol% MnO_2 and 0.5 mol% V_2O_5 cooled at 5°C min^{-1} . This particular sample also had a high E_{break} of 1330 V cm^{-1} and a low J_{leak} of $180 \mu\text{A cm}^{-2}$. It is apparent from Fig. 4 that the samples containing 0.5 mol% V_2O_5 produce the highest values of α , in agreement with the work of Kuo et al. on the binary V_2O_5 –ZnO system.⁹ We note that while the values of α that we have measured for these samples containing 0.5 mol% V_2O_5 are less than those recently reported by Hng and Chan,⁴ it is evident that acceptable varistor properties arise over a relatively wide composition field in this system when samples are cooled at 5°C min^{-1} after sintering. Furthermore, samples do not necessarily need to be slowly cooled at 5°C min^{-1} —faster cooling such as air cooling can also be used to produce successful varistors.

4. Conclusions

ZnO varistors have been prepared using ZnO with small quantities of V_2O_5 and MnO_2 . It is apparent that acceptable varistor properties can be obtained within the range of doping of vanadium and manganese examined. The best varistor properties were found in samples containing 0.25 mol% MnO_2 and 0.5 mol% V_2O_5 cooled at 5°C min^{-1} .

Acknowledgements

H. Pfeiffer thanks Consejo Nacional de Ciencia y Tecnología (CONACyT) and Secretaría de Educación Pública (SEP) of México for financial support.

References

1. Clarke, D. R., Varistor ceramics. *J. Am. Ceram. Soc.*, 1999, **82**, 485–502.
2. Kuo, C. T., Chen, C. S. and Lin, I. N., Microstructure and non-linear properties of microwave-sintered ZnO– V_2O_5 varistors: II, Effect of Mn_3O_4 doping. *J. Am. Ceram. Soc.*, 1998, **81**, 2949–2956.
3. Hng, H. H. and Knowles, K. M., Microstructure and current-voltage characteristics of multicomponent vanadium-doped zinc oxide varistors. *J. Am. Ceram. Soc.*, 2000, **83**, 2455–2462.
4. Hng, H. H. and Chan, P. L., Effects of MnO_2 doping in V_2O_5 -doped ZnO varistor system. *Mater. Chem. Phys.*, 2002, **75**, 61–66.
5. Hng, H. H., Knowles, K. M. and Midgley, P. A., Zinc vanadates in vanadium oxide-doped zinc oxide varistors. *J. Am. Ceram. Soc.*, 2001, **84**, 435–441.

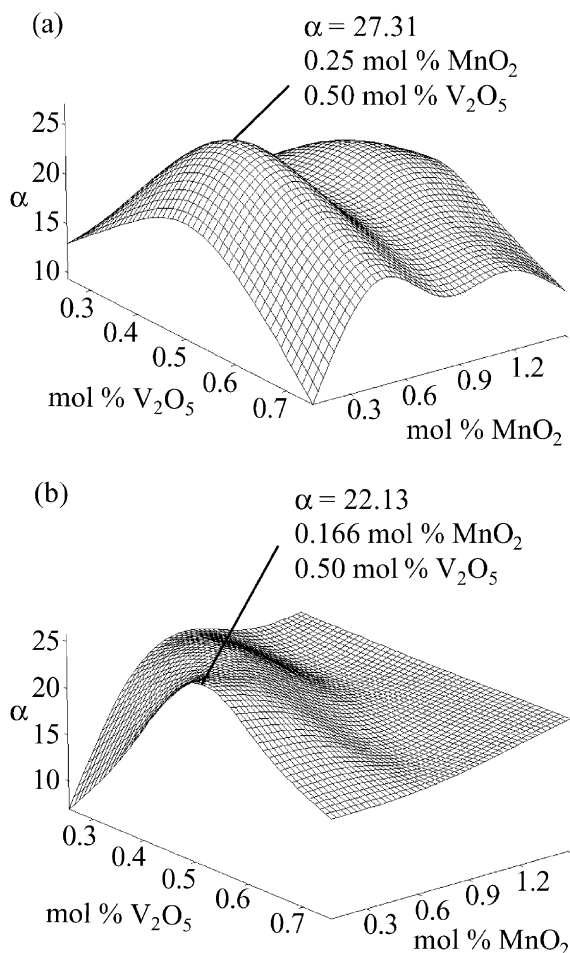


Fig. 4. Non-linear coefficient values, α , as a function of the V_2O_5 and MnO_2 concentrations: (a) samples cooled down from the sintering temperature at 5°C min^{-1} and (b) samples air cooled after sintering.

6. Brown, J. J. and Hummel, F. A., Reactions between ZnO and selected oxides of elements of groups IV and V. *Trans. Br. Ceram. Soc.*, 1965, **64**, 419–437.
7. Gopal, R. and Calvo, C., Crystal structure of α -Zn₃(VO₄)₂. *Can. J. Chem.*, 1973, **51**, 1004–1009.
8. Mendelson, M. I., Average grain size in polycrystalline ceramics. *J. Am. Ceram. Soc.*, 1969, **52**, 443–446.
9. Kuo, C. T., Chen, C. S. and Lin, I. N., Microstructure and non-linear properties of microwave-sintered ZnO–V₂O₅ varistors: I, effect of V₂O₅ doping. *J. Am. Ceram. Soc.*, 1998, **81**, 2942–2948.